Carbohydrate Polymers 103 (2014) 566–572

Contents lists available at ScienceDirect

Carbohydrate Polymers

journal homepage: www.elsevier.com/locate/carbpol

Synthesis and characterization of PEG-conjugated quaternized chitosan and its application as a gene vector

Xi Zhang [a], Juan Yao [b], Lihong Zhang [a], Jianguo Fang [b], Fengling Bian [a,*]

[a] Key Laboratory of Nonferrous Metal Chemistry and Resources Utilization of Gansu Province, College of Chemistry and Chemical Engineering, Lanzhou University, Lanzhou 730000, China
[b] State Key Laboratory of Applied Organic Chemistry, Lanzhou University, Lanzhou 730000, China

ARTICLE INFO

Article history:
Received 21 September 2013
Received in revised form
23 December 2013
Accepted 25 December 2013
Available online 3 January 2014

Keywords:
Chitosan
Quaternization
PEGylation
Nanocomplexes
Gene vector

ABSTRACT

Poly(ethylene glycol)-conjugated *N*-(2-hydroxy) propyl-3-trimethyl ammonium chitosan chloride (PHTAC) derivatives were prepared by incorporating PEG molecules onto quaternized chitosan backbone. The copolymers were characterized by FTIR, ^{1}H NMR and XRD. Agarose gel retardation assay indicated that PHTAC had good plasmid DNA (pDNA) binding capability and the particle sizes of PHTAC/pDNA complexes determined by DLS were about 200 nm. Cytotoxicity assays in HeLa and 293T cells showed that PHTAC had low cytotoxicity. In vitro luciferase assay showed that PHTAC with PEGylation degree of 9% (PHTAC-1) had good transfection efficiency about 5.3-fold higher than quaternized chitosan, which was comparable with PEI (25 kDa). These results suggest that PHTAC-1 is a promising candidate as an efficient nonviral gene vector.

1. Introduction

Gene therapy has developed rapidly in recent years (Green, Langer, & Anderson, 2008; Verma & Somia, 1997). As the prerequisite of successful gene transfer, a suitable gene vector needs to be safe and efficient. Among various vectors, cationic polymers possess capabilities to form compact complexes with DNA and induce efficient cell uptake and endosomal escape, thus have been an intriguing interest for researchers (Guo & Huang, 2012; Zhang, Zhao, Zhao, & Wang, 2010).

Chitosan is a natural polysaccharide possessing biocompatibility, biodegradability and low toxicity, and has been employed in gene delivery (Merkel, Zheng, Debus, & Kissel, 2012; Muzzarelli, 2010a). However, the poor solubility in physiological pH significantly limits its further application as an effective gene carrier. Quaternization, one of the common strategies to improve the performance of chitosan, can improve DNA binding capability of chitosan. In addition, cellular uptake capacity can be facilitated through the electrostatic affinity between quaternized chitosan and cell membranes, which is helpful to better transfection efficiency (Mao et al., 2007; Thanou, Florea, Geldof, Junginger, & Borchard, 2002). Xiao et al. (2012) reported that *N*-(2-hydroxy) propyl-3-trimethyl ammonium chitosan chloride was more efficient in transfection efficiency than chitosan in HeLa cells, ranging from 12.6-fold to 584.2-fold. Faizuloev et al. (2012) discovered that quaternized chitosan with degree of quaternization 90 ± 3% was 4-fold more efficient than PEI (25 kDa) in gene transfection efficiency. Xiao et al. (2013) found that in HepG2 cells galactosylation of quaternized chitosan yielded significant higher transfection efficiency than galactosylated chitosan.

However, higher quaternization degrees tend to have apparent cytotoxicity and excessive DNA condensing capacity, which deter DNA dissociation and limit the gene expression level (Faizuloev et al., 2012; Kean, Roth, & Thanou, 2005; Xiao et al., 2012). Thus further effort is still needed to improve the performance of quaternized chitosan.

PEG has unique physical characteristics and biological properties, which leads it a valid element employing in gene delivery (Pasut & Veronese, 2012). PEG modification can alter the physical properties of polymer/pDNA complexes and reduce the cytotoxicity of polymers. Besides, PEGylation is deemed to enhance colloidal stability and maintain polyplex sizes under different conditions, potentially resulting in increased cell uptake efficiency in vitro (Germershaus, Mao, Sitterberg, Bakowsky, & Kissel, 2008).

Therefore, the current investigation aims at combining the advantages of quaternization and PEGylation of chitosan while minimizing the short-comings. Based on theses purposes, three PHTAC copolymers with different PEGylation degrees were

* Corresponding author. Tel.: +86 931 8912582; fax: +86 931 8912582.
E-mail address: bianfl@lzu.edu.cn (F. Bian).

0144-8617/$ – see front matter © 2013 Elsevier Ltd. All rights reserved.
http://dx.doi.org/10.1016/j.carbpol.2013.12.072

synthesized. PHTAC/pDNA complexes were prepared and characterized in terms of DNA condensation efficiency, particle size, zeta potential, cell viability and in vitro transfection efficiency.

2. Materials and methods

2.1. Materials

Higher molecular weight chitosan was purchased from Golden shell Biochemical Co. Ltd. (Zhejiang, China). Polyethylenimine (PEI; branched, M_w = 25 kDa), *N*-hydroxysuccinimide (NHS), *N*,*N*′-dicyclohexylcarbodiimide (DCC) and 3-(4,5-dimethylthiazol-2-yl)-2,5-diphenyltetrazolium bromide (MTT) were obtained from Sigma Aldrich. Poly(ethylene glycol) monomethylether (mPEG; M_w = 1.9 kDa) was purchased from Alfa Aesar. Glycidyl trimethylammonium chloride (GTA) was obtained from Dongying Guofeng Fine Chemical Co. Ltd. (Shandong, China). Dulbecco's Modified Eagle's Medium (DMEM) and fetal bovine serum (FBS) were obtained from Invitrogen. All other chemicals were of analytical grade and were used as received unless otherwise specified.

2.2. Depolymerization of chitosan

Chitosan was depolymerized according to the literature (Mao et al., 2004; Muzzarelli, 2009, 2010b). The degree of deacetylation was measured by potentiometric titration as 85% and the molecular weight was determined by the intrinsic viscosity method using 2% HAc/0.2 M NaAc as solvent system. Data were obtained at 25 ± 0.05 °C in triplicate. The viscosity–average molecular weight (M_w) of chitosan was calculated as 120 kDa using Mark–Houwink equation:

$$[\eta] = KM_w{}^{\alpha}$$

where $[\eta]$ is the intrinsic viscosity, K and α are constants for given solute–solvent system and temperature, which are determined as 1.38×10^{-5} and 0.85 respectively by the literature (Kasaai, Arul, & Charlet, 2000).

2.3. Synthesis of N-(2-hydroxy) propyl-3-trimethyl ammonium chitosan chloride (HTAC)

HTAC was prepared by a modified method of Lim and Hudson (2004). 1 g of chitosan was dispersed in 20 mL of deionized water. After stirring at 85 °C for 30 min, 1.8 mL of GTA solution (1 g/mL) was added dropwise into the mixture. The reaction mixture was further stirred for 10 h at the same temperature. After using acetone to precipitate the product, the light yellow product was collected and washed by acetone several times. Then the collected product was dissolved in distilled water and dialyzed (MWCO = 3500) against distilled water for 5 days and finally lyophilized.

2.4. Synthesis of N-hydroxysuccinimide terminated poly(ethylene glycol) (NHS-mPEG)

NHS-mPEG was prepared according to the literature (Mao et al., 2005). Briefly, 2.5 g (1.3 mmol) of pre-dried mPEG was dissolved in 20 mL of anhydrous toluene, and 0.64 g of maleic anhydride (6.5 mmol) was added under argon protection. The mixture was stirred for 48 h at 70 °C under argon atmosphere. Then toluene and excess maleic anhydride were removed by distillation and sublimation under vacuum. After that, the above intermediate (0.54 mmol) and NHS (2.7 mmol) were dissolved together in 20 mL of anhydrous dichloromethane. Then the flask was cooled by ice-water bath and DCC (0.54 mmol) was added under protection of argon. After sealing the flask, the reaction mixture was stirred for 1 h in ice-water bath, and further 24 h at room temperature. The 1,3-dicyclohexylurea precipitation was eliminated by filtration. The filtrate was then added to 50 mL of diethyl ether and cooled for 2 h at 4 °C. The precipitated product was purified by redissolving in dichloromethane and reprecipitating with diethyl ether for three times. Finally, the product obtained by vacuum drying was stored under argon protection at room temperature.

Table 1
Properties of PHTAC copolymers.

Samples	NHS-mPEG/HTAC (w/w)	DQ[a] (%)	DP[b] (%)
PHTAC-1	2.5:1	41	9
PHTAC-2	5.0:1	41	13
PHTAC-3	7.5:1	41	27

[a] Number of quaternary ammonium groups per glucosamine unit, determined by ^{1}H NMR data.
[b] Number of PEG chains per glucosamine unit, determined by ^{1}H NMR data.

2.5. Synthesis of poly(ethylene glycol)-conjugated HTAC (PHTAC)

HTAC was dissolved in deionized water (10 mg/mL) and NHS-mPEG was dissolved in anhydrous DMSO (50 mg/mL). Then appropriate volumes of the above two solutions were mixed and stirred for 24 h at room temperature. As shown in Table 1, the weight ratios of HTAC to NHS-mPEG were varied to obtain three samples with different degrees of PEGylation (DP). After stirring for 24 h, the solution was dialyzed (MWCO = 14,000) against distilled water for 5 days and lyophilized.

2.6. Characterization of polymers

Fourier transform infrared (FTIR) spectra were carried out with NEXUS670 FTIR spectroscopy (Nicolet, USA). The samples were mixed with KBr and KBr pallets were prepared for measurements.

The ^{1}H nuclear magnetic resonance (^{1}H NMR) spectra were determined on a Bruker AV-400 NMR spectrometer at 400 MHz using D_2O or $CDCl_3$ as solvents.

X-ray diffraction spectra of the samples in the powder form were performed by a X-ray scattering diffractometer (Shimadzu XRD-6000, Japan) with Cu Kα radiation (λ = 1.5444) in the range of 5–50° (2θ) at a voltage of 40 kV and a current of 40 mA.

2.7. Plasmid DNA preparation

The reporter plasmid encoding luciferase (pGL3-Control, Promega) was propagated in DH5-α *Escherichia coli* and purified by the EndoFree Plasmid Kit (Qiagen, German). The purity of plasmid DNA (pDNA) was checked by electrophoresis on a 1% agarose gel, and the concentration of DNA was determined by measuring the UV absorbance of 260 nm. The purified pDNA was resuspended in Tris–EDTA buffer (pH = 8) and stored at −20 °C.

2.8. Preparation of PHTAC/DNA complexes

PHTAC samples were dissolved in PBS buffer (pH 7.4) with a concentration of 1 mg/mL and then the solutions were filtered using a 0.22 μm filter. The pDNA stock solutions (0.1 mg/mL) were prepared in Tris–HCl buffer. Complexes were prepared by adding polymer solutions to equal volumes of pDNA solution (containing 1 μg pDNA) at various *N*/*P* ratios and vortexed for 30 s. The resulting complexes were incubated for 30 min at room temperature before use.

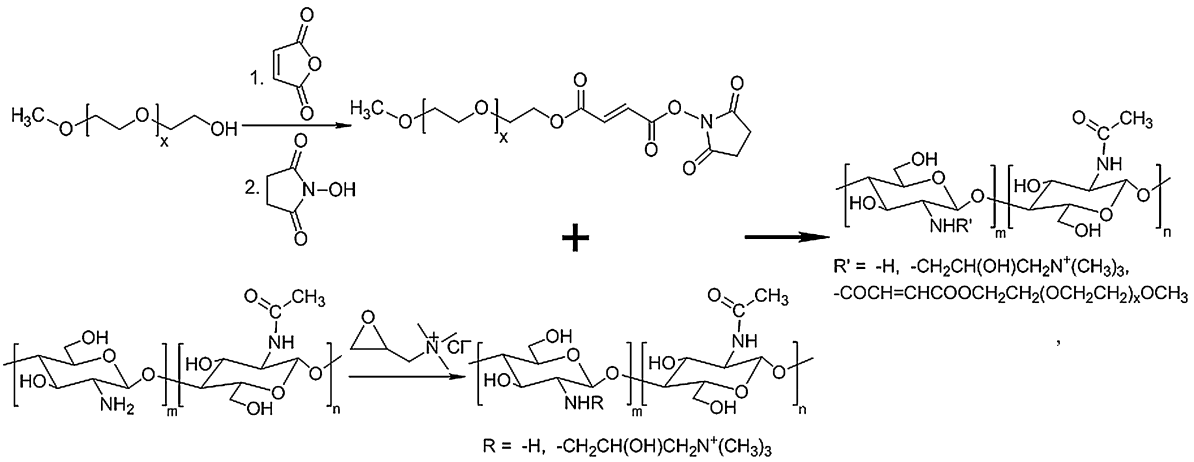

Scheme 1. Synthesis of poly(ethylene glycol)-conjugated *N*-(2-hydroxy) propyl-3-trimethyl ammonium chitosan chloride (PHTAC).

2.9. Agarose gel retardation assay

PHTAC copolymers were examined for their abilities to bind pDNA through gel electrophoresis experiments. The PHTAC/pDNA complexes with different *N*/*P* ratios ranging from 1.5 to 15 were formed according to the procedure described above. Then 10 μL of complexes suspension was electrophoresed on 1.0% (w/v) agarose gel containing ethidium bromide (0.5 μg/mL) with 1 × TAE running buffer (40 mM Tris-acetate, 1 mM EDTA) at 100 V for 30 min. The results were observed by irradiation under UV light.

2.10. Zeta potential and particle size measurement

The zeta potential and particle size were measured in triplicate by Zetasizer Nano ZS (Malvern Instruments, UK) at 25 °C. The PHTAC/pDNA complexes at various *N*/*P* ratios ranging from 1 to 9 were prepared by adding appropriate volumes of polymer solution to 1 μg of pDNA. The complexes solution was then incubated at room temperature for 30 min and diluted by PBS buffer for particle size measurement or diluted by distilled water for zeta-potential measurement to 1 mL prior to measurement.

2.11. Transmission electron microscopy

The morphologies of PHTAC/pDNA complexes (*N*/*P* = 9) were observed using a JEOL JEM-1230 transmission electron microscope (TEM). Briefly, a drop of the complexes was deposited on carbon-coated grids and dried at room temperature, and then the samples were examined with the electron telescope.

2.12. Cell culture

HeLa and 293T cells were cultured in DMEM medium supplemented with 10% FBS and 1% penicillin–streptomycin at 37 °C in a humidified atmosphere containing 5% CO_2.

2.13. Evaluation of cytotoxicity

The cells were seeded in 96-well plates at a density of 1×10^4 cells/well and incubated for 24 h in 200 μL of DMEM containing 10% FBS. Media were replaced by 180 μL of fresh serum free DMEM media. And then 20 μL of filtered polymer solutions were added to achieve the final concentrations of 5, 25, 50, 100 and 200 μg/mL. After 24 h of incubation, 20 μL of MTT solution (5 mg/mL, in PBS buffer) was added and further incubated at 37 °C for 4 h. Thereafter, the media were removed and 150 μL of DMSO was added to each well to dissolve the formazan crystals. Absorbance was measured at 570 nm using a microplate reader (Infinite M200, TECAN). The cell viability (%) was calculated according to the following equation:

$$\text{Cell viability}(\%) = \frac{OD_{570(\text{sample})}}{OD_{570(\text{control})}} \times 100$$

where $OD_{570(\text{sample})}$ is obtained from the wells treated with the samples, and $OD_{570(\text{control})}$, from the wells treated only with PBS buffer.

2.14. In vitro transfection

293T cells were seeded in 24-well plates at an initial density of 6×10^4 cell/well and allowed to reach 70–80% confluence. Prior to transfection, the cells were washed with PBS and refreshed with serum-free medium. Then the cells were treated with complexes containing 1 μg of pDNA at various *N*/*P* ratios and incubated for 4 h. After that, cells were refreshed with complete medium and cultured for another 48 h. Next, the medium was removed and the cells were rinsed by PBS and lysed by 200 μL of lysis buffer (Promega, USA). Then the lysate was harvested and centrifuged. 20 μL of the cell lysate was incubated with 100 μL of luciferin substrate (Promega, USA) and the luciferase activity was measured by detecting the light emission in a luminometer (Lumat LB9507, Berthold). The protein content of the cell lysate was determined by BCA protein assay kit (Pierce, USA). The results are denoted as relative light units per milligram of cell protein lysate (RLU/mg protein).

3. Results and discussion

3.1. Synthesis and characterization of PHTAC

PHTAC was prepared through PEGylation of quaternized chitosan as illustrated in Scheme 1. The amine groups of chitosan were first reacted with epoxy groups of GTA. Then, the copolymers were obtained by the reaction of NHS-mPEG and quaternized chitosan under the presence of DCC/NHS. The reaction conditions are shown in Table 1 and PHTAC copolymers with different degrees of PEGylation are denoted as PHTAC-1, PHTAC-2 and PHTAC-3.

Chitosan (a), HTAC (b) and PHTAC-1 (c) were first characterized by FTIR spectroscopy, as shown in Fig. 1. In Fig. 1(a), the band at 3436 cm^{-1} was attributed to N—H and O—H stretching vibrations. The bands at 2876 cm^{-1} and 1603 cm^{-1} corresponded to C—H and N—H stretching vibrations respectively. The characteristic peaks of C—O—C anti-symmetric stretching vibration and C—O

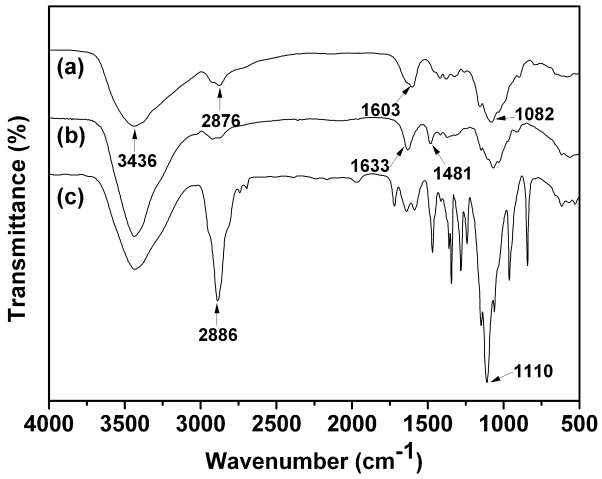

Fig. 1. FTIR spectra of chitosan (a), HTAC (b) and PHTAC-1 (c).

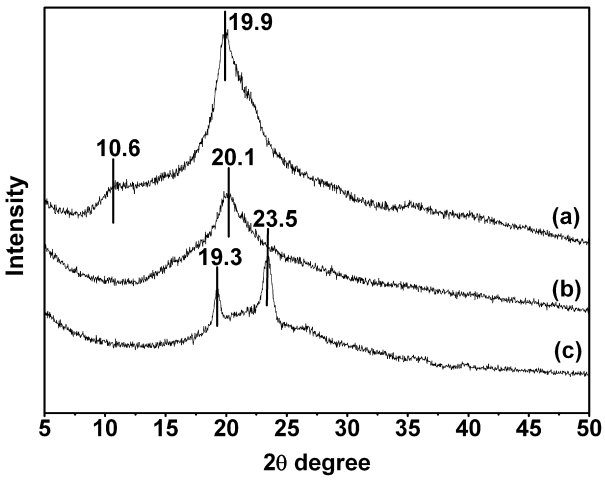

Fig. 3. X-ray diffractograms of chitosan (a), HTAC (b) and PHTAC-1 (c).

stretching vibration could be viewed at 1156 cm^{-1} and 1082 cm^{-1} (Liu et al., 2012). Comparing with chitosan, several changes were found in the spectrum of HTAC. The new band at 1481 cm^{-1} was attributed to C—H stretching vibration of quaternary ammonium groups. The band of primary amine at 1603 cm^{-1} disappeared and a new peak appeared at 1633 cm^{-1} corresponding to secondary amine in Fig. 1(b), which denoted the reaction of NH_2 sites on the chitosan backbone (Xiao et al., 2012). After reaction of HTAC and NHS-mPEG, the significant increase of the intensity of peaks at 2886 cm^{-1} and 1110 cm^{-1} could be attributed to C—H stretching vibration of repeat units (—CH_2CH_2O—) and C—O—C vibration of PEG chains (Cui, Tang, & Yin, 2012), which confirmed the synthesis of PHTAC-1.

The ^{1}H NMR spectra of HTAC (a), NHS-mPEG (b) and PHTAC-1 (c) are shown in Fig. 2. As shown in Fig. 2(a), the peak at 3.2 ppm was attributed to hydrogen of quaternary ammonium groups. By comparing with the intensity of peaks at 3.4–4.3 ppm (multiplet, assigned to glucosamine unit, H-3, H-4, H-5, H-6, H-6′), the quaternization degree (DQ) was calculated as 41% per glucosamine unit in HTAC. The characteristic signals in Fig. 2(b) verified the structure of NHS-mPEG, which is in accordance with the report (Mao et al., 2005). After the reaction of NHS activated mPEG and HTAC, the peaks of mPEG (—CH=CH—) appeared at 6.5 and 6.9 ppm in Fig. 2(c), indicating that PEG was conjugated to HTAC. The PEGylation degree (DP) was determined by comparing the signal integrals of —CH=CH— with integrals of quaternary ammonium group signals. The PEGylation degrees were calculated as 9%, 13% and 27% for PHTAC-1, PHTAC-2 and PHTAC-3.

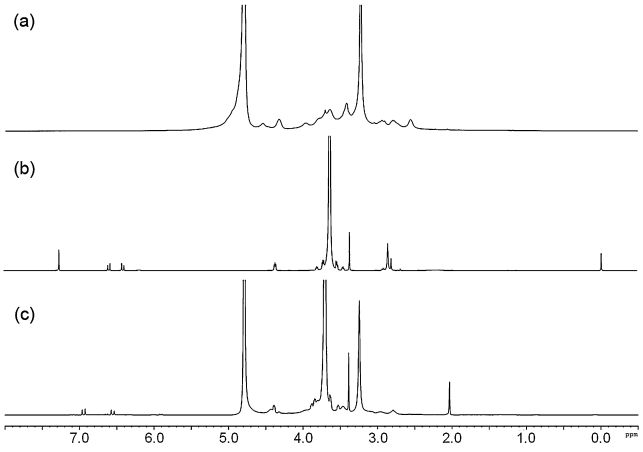

Fig. 2. ^{1}H NMR spectra of HTAC (a), NHS-mPEG (b) and PHTAC-1 (c).

The X-ray diffractograms of chitosan (a), HTAC (b) and PHTAC-1 (c) are shown in Fig. 3. It could be found that chitosan showed two different characteristic peaks at 10.6° and 19.9°, which were assigned to hydrated crystal and regular crystalline lattice (1 1 0) respectively (Harish Prashanth, Kittur, & Tharanathan, 2002). In Fig. 3(b), the peak at 10.6° disappeared and the peak at 19.9° decreased significantly and moved to a higher 2θ at 20.1°. This fact may be explained by the destruction of intermolecular hydrogen bond due to modification of NH_2 on chitosan (Xiao et al., 2012). Comparing with HTAC, new peaks at 19.3° and 23.5° appeared in the XRD spectrum of PHTAC-1, which was attributed to PEG chains on chitsoan backbone (Cui et al., 2012).

3.2. Agarose gel retardation assay

DNA condensation ability is a fundamental requirement for gene vectors. The ability of PHTAC to form complexes with pDNA was evaluated by agarose gel retardation assay. As shown in Fig. 4, the migrations of pDNA in agarose gel were completely retarded when the *N*/*P* ratios were higher than 1.5 for PHTAC-1 and PHTAC-2, indicating that they could bind DNA strongly. However, the pDNA was absolutely retarded when *N*/*P* ratio of PHTAC-3 was above 3, which is related to the weaker electrostatic interactions between PHTAC-3 and pDNA (Huang et al., 2010).

3.3. Particle size, zeta potential and morphology of the complexes

Appropriate size is an important factor to ensure the cellular uptake of the polymer/pDNA complexes. It is reported that the cells usually uptake particles ranging from about 50 to several hundred nanometers (Liu & Reineke, 2005). The sizes of the PHTAC/pDNA complexes at different *N*/*P* ratios were measured by dynamic light scattering (DLS). As shown in Fig. 5a, the diameters of the PHTAC/pDNA complexes decreased with the increasing *N*/*P* ratios. When the *N*/*P* ratios increased from 1 to 3, the sizes of the complexes decreased significantly and approached a plateau of about 200 nm at the *N*/*P* ratios more than 6. The net electrostatic repulsive force at high *N*/*P* ratios has the ability to prevent aggregation of complexes, which in further stabilizes nanoparticles (Jiang et al., 2007; Wong et al., 2006).

Positive surface charge of the complexes is known to be one of the major factors influencing cell internalization and transfection efficiency. The zeta potentials of the complexes at various *N*/*P* ratios

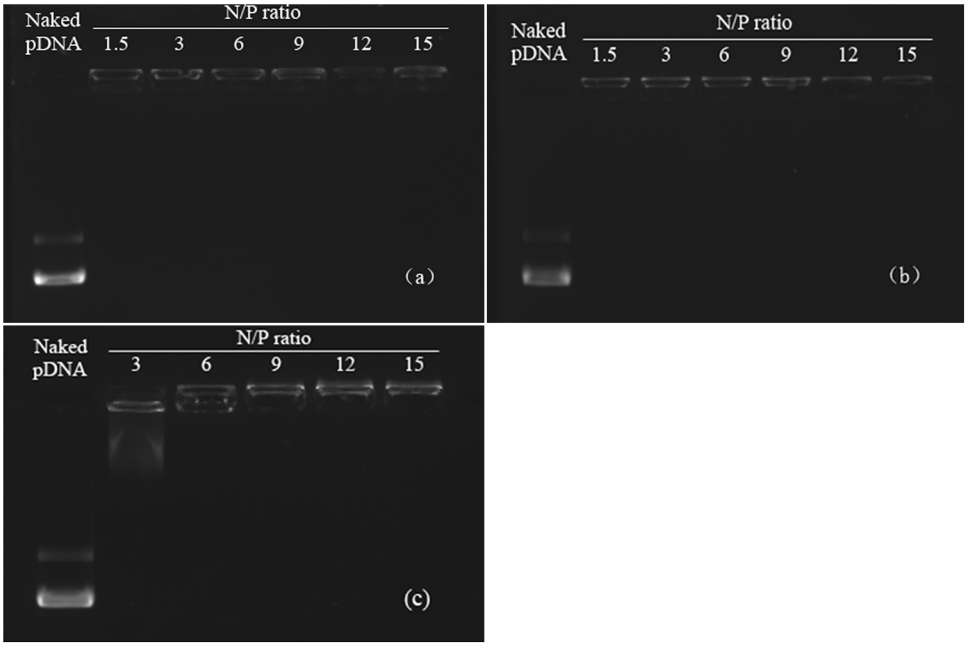

Fig. 4. Agarose gel electrophoresis of polymer/pDNA complexes formed by PHTAC-1 (a), PHTAC-2 (b) and PHTAC-3 (c) at various *N*/*P* ratios.

are shown in Fig. 5b. The zeta potentials of PHTAC/pDNA complexes increased with *N*/*P* ratios. When *N*/*P* ratios were above 6, the zeta potentials approached plateaus about 26 mV, 20 mV and 8 mV for PHTAC-1, PHTAC-2 and PHTAC-3 respectively due to the saturation of polycations complexed with pDNA. Besides, the zeta potentials were found to diminish with higher DP, which could be attributed to the stronger shielding effect of PEG chains on the surface of the complexes (Le lu, Strand, Steine, & de Lange Davies, 2011).

The morphologies of PHTAC/pDNA complexes were observed by TEM. As shown in Fig. 5c, the typical images indicated that most of the PHTAC/pDNA complexes had spherical shapes and they were finely dispersed in the field of vision. Moreover, the TEM images demonstrated that the sizes of the nanoparticles formed by PHTAC with different DP had no apparent difference and were all less than 100 nm, which were smaller than the results of DLS. The possible reason is that the particles are highly swollen in solution for DLS

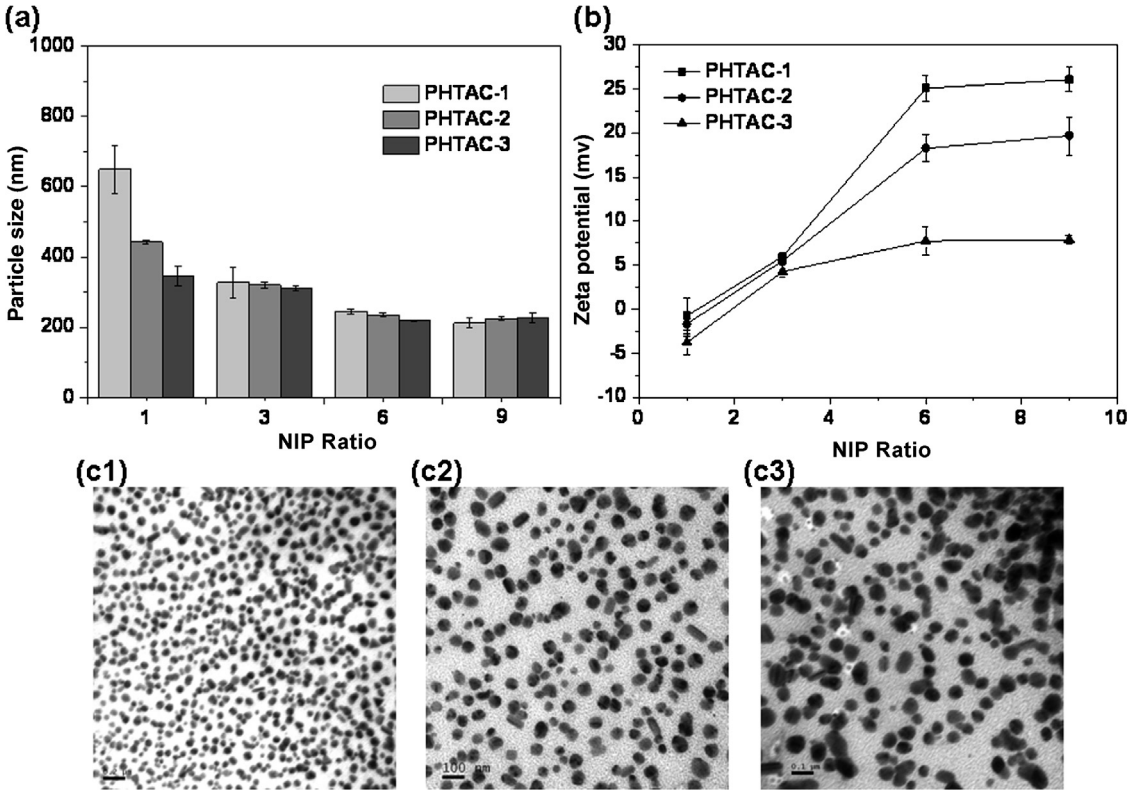

Fig. 5. Particle size (a) and zeta potential (b) of PHTAC/pDNA complexes at various *N*/*P* ratios. Data are presented as mean ± standard deviation ($n = 3$). The TEM images of polymer/pDNA complexes at *N*/*P* ratios of 9 formed by PHTAC-1 (c1), PHTAC-2 (c2) and PHTAC-3 (c3). Scale bar is 0.2 μm (c1), 0.1 μm (c2) and 0.1 μm (c3) respectively.

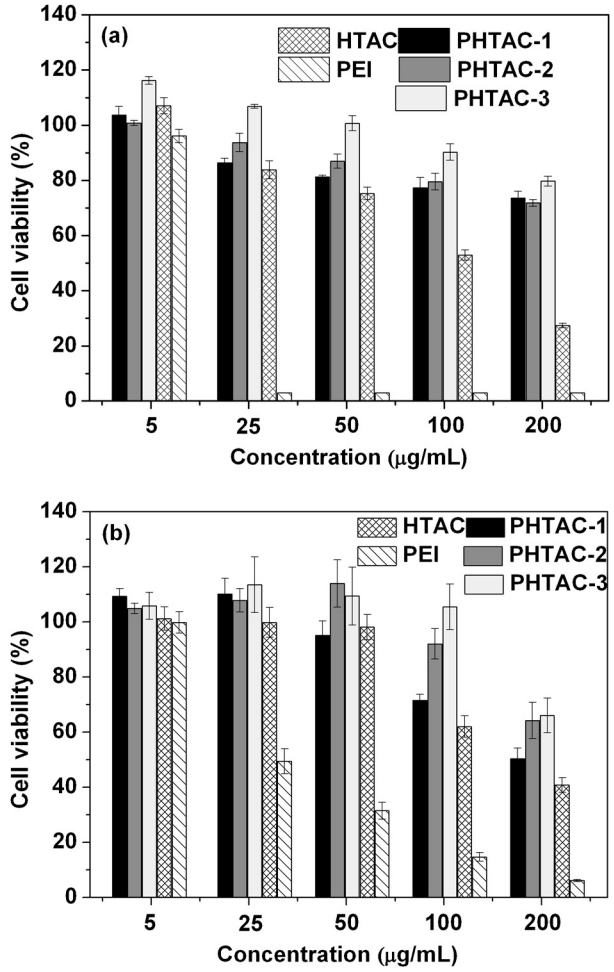

Fig. 6. Cytotoxicity of HTAC and PHTAC compared with PEI (25 kDa) at various concentrations in HeLa (a) and 293T (b) cells. Data are presented as mean ± standard deviation ($n = 5$).

measurements while they are dried at room temperature for the examination of TEM (Xiao et al., 2013).

3.4. Cytotoxicity of PHTAC

The cytotoxicities of HTAC and PHTAC in HeLa and 293T cell lines were evaluated by MTT assay, PEI (25 kDa) was used as a control. As shown in Fig. 6, it was found that the cytotoxicities of all polymers were increasing with higher concentrations. Compared with PEI (25 kDa), which owned the highest cytotoxicity among all the tested samples, the chitosan derivatives had less cytotoxicity. Furthermore, all of the PHTAC copolymers were less toxic than HTAC in both cell lines tested. It is reported that the cytotoxicity of cationic polymers is probably caused by the interactions with the plasma membrane or negatively charged cell components and proteins (Choksakulnimitr, Masuda, Tokuda, Takakura, & Hashida, 1995; Fischer, Li, Ahlemeyer, Krieglstein, & Kissel, 2003). In the present work, after PEG molecules were conjugated to HTAC, they would provide steric repulsion which results in partly shielding of positive charges on HTAC (Zhu, Qian, Zhang, Tang, & Yin, 2007). PHTAC-1, PHTAC-2 and PHTAC-3 had increasing DP, leading to decreasing surface charge, which was in accordance with the decreasing tendency of cytotoxicity.

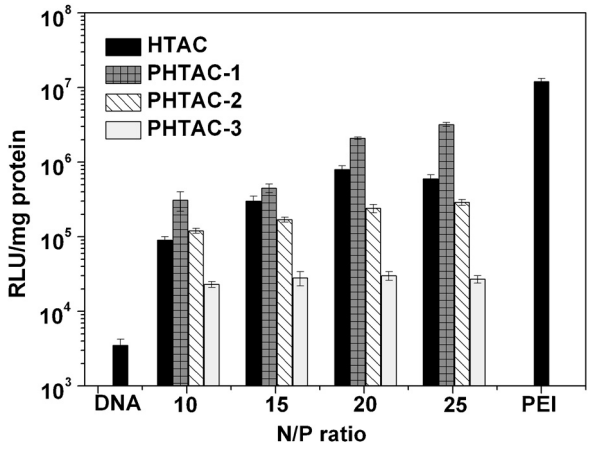

Fig. 7. In vitro gene transfection efficiency of polymer/pDNA complexes formed by HTAC and PHTAC compared with PEI (25 kDa) at N/P ratio of 10 in 293T cells. Data are presented as mean ± standard deviation ($n = 3$).

3.5. In vitro transfection efficiency of the complexes

The in vitro gene transfer abilities of HTAC and PHTAC were investigated by pGL3-Control in 293T cell line using PEI (25 kDa) at its optimal ratio ($N/P = 10$) as the control. From Fig. 7, we can find that the transfection efficiencies increased with increasing N/P ratios for PHTAC, while the maximum transfection efficiency of HTAC/pDNA was observed at N/P ratio of 20 and tended to decrease with further increasing N/P ratio. It can be attributed that HTAC could strongly entangle pDNA through electrostatic interactions at high N/P ratio, and the strong interactions between pDNA and HTAC result in highly stable complexes, thereby preventing dissociation within the cell and ultimately precluding the translation of DNA.

Comparing with HTAC/pDNA complexes, PHTAC-1/pDNA yielded an increase in transfection efficiency at the range of 1.5-fold (at N/P ratio of 15) to 5.3-fold (at N/P ratio of 25). At its optimum N/P ratio, PHTAC-1 showed comparable gene transfer ability with PEI (25 kDa), which has been considered to be a highly effective cationic gene vector. The results demonstrate that appropriate amounts of PEGylation can improve the cytotoxicity and enhance the transfection activity as well.

However, PHTAC-2/pDNA and PHTAC-3/pDNA complexes had low efficiency, even less than that of HTAC/pDNA. The possible reason is that high DP excessively shields positive charges and obtains low zeta potentials of polymer/pDNA complexes, which affects the attachment of complexes to the cells and further leads to low transfection efficiency.

4. Conclusion

In summary, we have prepared three PHTAC copolymers by conjugating PEG with HTAC via amide bond. The effects of PEGylation degree on their physicochemical properties have been investigated in details. These polymers show good DNA binding ability, and the spherical PHTAC/pDNA nanoparticles have desired diameters of ~200 nm. These PHTAC copolymers with different DP exhibit lower cytotoxicity than HTAC. Among the complexes, PHTAC-1/pDNA complexes display the highest transfection efficiency, which is higher than that of HTAC/pDNA complexes. PHTAC-1's performance as a gene vector is comparable to branched PEI (25 kDa). These results may provide crucial information and insight for the future design of novel gene vector with excellent transfection efficiency.

Acknowledgment

This work was supported by the National Natural Science Foundation of China (No. 51273086) and the National Science Foundation for Fostering Talents in Basic Research of the National Natural Science Foundation of China (No. J1103307).

References

Choksakulnimitr, S., Masuda, S., Tokuda, H., Takakura, Y., & Hashida, M. (1995). In vitro cytotoxicity of macromolecules in different cell culture systems. *Journal of Controlled Release*, *34*, 233–241.

Cui, L. M., Tang, C., & Yin, C. H. (2012). Effects of quaternization and PEGylation on the biocompatibility, enzymatic degradability and antioxidant activity of chitosan derivatives. *Carbohydrate Polymers*, *87*, 2505–2511.

Faizuloev, E., Marova, A., Nikonova, A., Volkova, I., Gorshkova, M., & Izumrudov, W. (2012). Water-soluble N-[(2-hydroxy-3-trimethylammonium) propyl] chitosan chloride as a nucleic acids vector for cell transfection. *Carbohydrate Polymers*, *89*, 1088–1094.

Fischer, D., Li, Y. X., Ahlemeyer, B., Krieglstein, J., & Kissel, T. (2003). In vitro cytotoxicity testing of polycations: Influence of polymer structure on cell viability and hemolysis. *Biomaterials*, *24*, 1121–1131.

Germershaus, O., Mao, S. R., Sitterberg, J., Bakowsky, U., & Kissel, T. (2008). Gene delivery using chitosan, trimethyl chitosan or polyethylenglycol-graft-trimethyl chitosan block copolymers: Establishment of structure–activity relationships in vitro. *Journal of Controlled Release*, *125*, 145–154.

Green, J. J., Langer, R., & Anderson, D. G. (2008). A combinatorial polymer library approach yields insight into nonviral gene delivery. *Accounts of Chemical Research*, *41*, 749–759.

Guo, X., & Huang, L. (2012). Recent advances in nonviral vectors for gene delivery. *Accounts of Chemical Research*, *45*, 971–979.

Harish Prashanth, K. V., Kittur, F. S., & Tharanathan, R. N. (2002). Solid state structure of chitosan prepared under different N-acetylating conditions. *Carbohydrate Polymers*, *50*, 27–33.

Huang, F. W., Wang, H. Y., Li, C., Wang, H. F., Sun, Y. X., Feng, J., et al. (2010). PEGylated PEI-based biodegradable polymers as non-viral gene vectors. *Acta Biomaterialia*, *6*, 4285–4295.

Jiang, H. L., Kim, Y. K., Arote, R., Nah, J. W., Cho, M. H., Choi, Y. J., et al. (2007). Chitosan-graft-polyethylenimine as a gene carrier. *Journal of Controlled Release*, *117*, 273–280.

Kasaai, M. R., Arul, J., & Charlet, G. (2000). Intrinsic viscosity–molecular weight relationship for chitosan. *Journal of Polymer Science. Part B: Polymer Physics*, *38*, 2591–2598.

Kean, T., Roth, S., & Thanou, M. (2005). Trimethylated chitosans as non-viral gene delivery vectors: Cytotoxicity and transfection efficiency. *Journal of Controlled Release*, *103*, 643–653.

Le lu, S., Strand, S. P., Steine, J., & de Lange Davies, C. (2011). Effect of PEGylation on the diffusion and stability of chitosan–DNA polyplexes in collagen gels. *Biomacromolecules*, *12*, 3656–3665.

Lim, S. H., & Hudson, S. M. (2004). Synthesis and antimicrobial activity of a water-soluble chitosan derivative with a fiber-reactive group. *Carbohydrate Research*, *339*, 313–319.

Liu, Y., & Reineke, T. M. (2005). Hydroxyl stereochemistry and amine number within poly(glycoamidoamine)s affect intracellular DNA delivery. *Journal of the American Chemical Society*, *127*, 3004–3015.

Liu, X. F., Zhi, X. N., Liu, Y. F., Wu, B., Sun, Z., & Shen, J. (2012). Effect of chitosan, O-carboxymethyl chitosan, and N-[(2-Hydroxy-3-N,N-dimethylhexadecyl ammonium) propyl] chitosan chloride on overweight and insulin resistance in a murine diet-induced obesity. *Journal of Agricultural and Food Chemistry*, *60*, 3471–3476.

Mao, S. R., Shuai, X. T., Unger, F., Simon, M., Bi, D. Z., & Kissel, T. (2004). The depolymerization of chitosan: Effects on physicochemical and biological properties. *International Journal of Pharmaceutics*, *281*, 45–54.

Mao, S. R., Shuai, X. T., Unger, F., Wittmar, M., Xie, X. L., & Kissel, T. (2005). Synthesis, characterization and cytotoxicity of poly(ethylene glycol)-graft-trimethyl chitosan block copolymers. *Biomaterials*, *26*, 6343–6356.

Mao, Z. W., Ma, L., Jiang, Y., Yan, M., Gao, C. Y., & Shen, J. C. (2007). N,N,N-trimethylchitosan chloride as a gene vector: Synthesis and application. *Macromolecular Bioscience*, *7*, 855–863.

Merkel, O. M., Zheng, M. Y., Debus, H., & Kissel, T. (2012). Pulmonary gene delivery using polymeric nonviral vectors. *Bioconjugate Chemistry*, *23*, 3–20.

Muzzarelli, R. A. A. (2009). Chitins and chitosans for the repair of wounded skin, nerve, cartilage and bone. *Carbohydrate Polymers*, *76*, 167–182.

Muzzarelli, R. A. A. (2010a). Chitins and chitosans as immunoadjuvants and non-allergenic drug carriers. *Marine Drugs*, *8*(2), 292–312.

Muzzarelli, R. A. A. (2010b). Chitosans: New vectors for gene therapy. In R. Ito, & Y. Matsuo (Eds.), *Handbook of carbohydrate polymers: Development, properties and applications* (pp. 583–604). New York: Nova Science Publishers, Inc.

Pasut, G., & Veronese, F. M. (2012). State of the art in PEGylation: The great versatility achieved after forty years of research. *Journal of Controlled Release*, *161*, 461–472.

Thanou, M., Florea, B. I., Geldof, M., Junginger, H. E., & Borchard, G. (2002). Quaternized chitosan oligomers as novel gene delivery vectors in epithelial cell lines. *Biomaterials*, *23*, 153–159.

Verma, I. M., & Somia, N. (1997). Gene therapy – Promises, problems and prospects. *Nature*, *389*, 239–242.

Wong, K., Sun, G. B., Zhang, X. Q., Dai, H., Liu, Y., He, C. B., et al. (2006). PEI-g-chtiosan, a novel gene delivery system with transfection efficiency comparable to polyethylenimine in vitro and after liver administration in vivo. *Bioconjugate Chemistry*, *17*, 152–158.

Xiao, B., Wan, Y., Wang, X. Y., Zha, Q. C., Liu, H. M., Qiu, Z. Y., et al. (2012). Synthesis and characterization of N-(2-hydroxy)propyl-3-trimethyl ammonium chitosan chloride for potential application in gene delivery. *Colloids and Surfaces B: Biointerfaces*, *91*, 168–174.

Xiao, B., Wang, X. Y., Qiu, Z. Y., Ma, J., Zhou, L., Wan, Y., et al. (2013). A dual-functionally modified chitosan derivative for efficient liver targeted gene delivery. *Journal of Biomedical Materials Research A*, *101*, 1888–1897.

Zhang, S. B., Zhao, Y. N., Zhao, B. D., & Wang, B. (2010). Hybrids of nonviral vectors for gene delivery. *Bioconjuate Chemistry*, *21*, 1003–1009.

Zhu, S. Y., Qian, F., Zhang, Y., Tang, C., & Yin, C. H. (2007). Synthesis and characterization of PEG modified N-trimethylaminoethylmethacrylate chitosan nanoparticles. *European Polymer Journal*, *43*, 2244–2253.